THE FASEB JOURNAL • RESEARCH • www.fasebj.org

Maternal obesity impairs fetal cardiomyocyte contractile function in sheep

Qiurong Wang,[*,†] Chaoqun Zhu,[†] Mingming Sun,[†] Rexiati Maimaiti,[†] Stephen P. Ford,[*,†,1] Peter W. Nathanielsz,[*,†] Jun Ren,[‡] and Wei Guo[*,†,‡,2]

[*]Center for the Study of Fetal Programming, [†]Animal Science Department, and [‡]Center for Cardiovascular Research and Alternative Medicine, University of Wyoming, Laramie, Wyoming, USA

ABSTRACT: Obesity is a major public health problem worldwide. In the United States, one-third of women of reproductive age are obese. Human studies show that maternal obesity (MO) predisposes offspring to cardiovascular disease. However, the underlying mechanisms remain unclear. Given the similarities between pregnancy in sheep and humans, we studied sheep to examine the impact of MO on fetal cardiomyocyte contractility at term. We observed that MO impaired cardiomyocyte contractility by reducing peak shortening and shortening/relengthening velocity, prolonging time to relengthening. MO disrupted Ca^{2+} homeostasis in fetal cardiomyocytes, increasing intracellular Ca^{2+} and inducing cellular Ca^{2+} insensitivity. The Ca^{2+}-release channel was impaired, but Ca^{2+} uptake was unaffected by MO. The upstream kinases that phosphorylate the Ca^{2+}-release channel—ryanodine receptor-2, PKA, and calmodulin-dependent protein kinase II—were activated in MO fetuses. Contractile dysfunction was associated with an increased ratio of myosin heavy chain (MHC)-β to MHC-α and upregulated cardiac troponin (cTn)-T and tropomyosin, as well as cTn-I phosphorylation. In summary, this is the first characterization of the effects of MO on fetal cardiomyocyte contractility. Our findings indicate that MO impairs fetal cardiomyocyte contractility through altered intracellular Ca^{2+} handling, overloading fetal cardiomyocyte intracellular Ca^{2+} and aberrant myofilament protein composition. These mechanisms may contribute to developmental programming by MO of offspring cardiac function and predisposition to later life cardiovascular disease in the offspring.—Wang, Q., Zhu, C., Sun, M., Maimaiti, R., Ford, S. P., Nathanielsz, P. W., Ren, J., Guo, W. Maternal obesity impairs fetal cardiomyocyte contractile function in sheep. FASEB J. 33, 000–000 (2019). www.fasebj.org

KEY WORDS: cardiac programming · myofilament · Ca^{2+} sensitivity

Obesity is an exponentially increasing public health epidemic and economic burden worldwide (1–3). Currently, ~18–35% of pregnant women in the United States are obese (4, 5). Epidemiologic studies suggest that maternal obesity (MO) during pregnancy exhibits intergenerational effects by programming offspring (F1) to increased risk of obesity and cardiometabolic problems (6–9), including insulin resistance, heart disease, hypertension, and vascular dysfunction (10–14). Both maternal under- and overnutrition play important roles in programming fetal heart development and function (15–18). Several studies have shown that MO increases the risk of congenital heart defects and impairs F1 fetal diastolic function (19–23). Furthermore, impaired myocardial function, increased septal thickness, and lower left ventricle (LV) Doppler velocity have been reported in fetuses of human mothers with MO (24). In addition, MO has been shown to program F1 cardiac structure (25–27).

Multiple studies of fetal cardiovascular programming have been performed in rodent models (18, 25, 28–33). In addition to their many strengths, rodent models of fetal programming have some limitations related to differences between precocial and altricial species in the timing of developmental mechanisms that result in programming. A good example is the timing of the peripartal increase in the circulating glucocorticoids that are responsible for terminal differentiation of multiple organs (34). With reference to the cardiovascular system, rodent heart rates are much higher than those in sheep and primates, including humans. Therefore, studies in precocial species are necessary to enable translation to programming in human development. Sheep share many similarities with human pregnancy (*i.e.*, singleton gestation being the most common litter size, which is important in terms of the nutritional burden placed on the

ABBREVIATIONS: CaMKII, calmodulin-dependent protein kinaseII; cTn, cardiac troponin; FFI, Fura-2 fluorescence intensity; KB, Kraft-Brühe; LV, left ventricle; MHC, myosin heavy chain; MO, maternal obesity; NRC, National Research Council; PLN, phospholamban; PS, peak shortening; RyR2, ryanodine receptor 2; SR, sacroplasmic reticulum; Serca, sarco/endoplasmic reticulum Ca-ATPase; TPS, time to peak shortening; TR_{90}, time to 90% relengthening; WGA, wheat germ agglutinin

[1] Deceased.

[2] Correspondence: University of Wyoming, 1000 E. University Avenue, Laramie, WY 82071, USA. E-mail: wguo3@uwyo.edu

doi: 10.1096/fj.201800988R

This article includes supplemental data. Please visit *http://www.fasebj.org* to obtain this information.

mother; comparable maternal size and adiposity; maternal:fetal weight ratio; length of gestation, important in the duration of nutritional challenges; birth weight; similar organogenesis for major body systems; equivalent rates of prenatal protein accretion and fat deposition; and relative maturity at birth) (35–43). Thus, a sheep MO model has unique potential for the study of the effects of MO programming on the fetal heart.

We have developed and characterized a diet-based sheep model of MO. Nulliparous ewes were fed an obesogenic diet at 150% National Research Council (NRC) recommendations (44) or a control diet at 100% NRC recommendations from 60 d before conception throughout gestation. To the best of our knowledge, this is the only sheep model of overnutrition programming by obesity that begins before pregnancy and thus parallels obesity, which is almost always present in women before pregnancy. This model has been well characterized. During the entire period of pregnancy, MO ewes gain a mean of 65–70% of their initial body weight, whereas control ewes gain only 15–20% (16, 45–47). At midgestation, fetuses of obese mothers exhibit a weight gain 30% greater than controls, altered organ growth and development, and increased adiposity in combination with elevated plasma glucose and insulin levels (47, 48). From mid to late gestation, ventricular weight, LV and right ventricle free wall weights, and LV wall thickness of fetuses of obese ewes increase compared with fetuses of control ewes (15, 49, 50). By late gestation, fibrosis and increased fetal heart connective tissue accumulation, associated with an upregulated TGF-β/p38 signaling pathway, are obvious in the MO fetal sheep myocardium (50). Furthermore, MO induces irregular myofiber orientation, increases interstitial space, and increases lipid droplet accumulation in fetal ventricular tissue, with upregulated levels of proinflammatory mediators (51). Despite the thicker wall and morphologic changes, MO fetal heart function is compromised, with impaired cardiac reserve when afterload is increased (16).

Despite the extensive characterization of this model, the molecular and cellular mechanisms causing compromised heart function in fetuses of MO mothers remain unclear. To rectify this deficiency, we studied the impact of MO on fetal cardiomyocyte contractile function and the underlying molecular mechanisms. We assessed contractility and intracellular Ca^{2+} handling in isolated LV cardiomyocytes from fetuses of normal-weight ewes (control group) and MO ewes (obese group). Cellular and molecular mechanisms that potentially govern contractile function were examined with a focus on intracellular Ca^{2+} handling and contractile and regulatory proteins in the sarcomere.

MATERIALS AND METHODS

Experimental animals

Nulliparous Rambouillet/Columbia crossed ewes obtained from the University of Wyoming Animal Science flock were fed either a highly palatable diet at 100% of NRC (44) recommendations (control) or 150% of NRC recommendations (MO) from 60 d before and throughout pregnancy. Water was available at all times. At gestational d135 (0.9 gestation; term 145 d), fetuses were delivered by C-section from ewes under general anesthesia initiated with ketamine (10 mg/kg) followed by isoflurane inhalation general anesthesia (2.5%) and euthanized by exsanguination, while the ewes and fetuses were still under general anesthesia. Ewes were then euthanized with an overdose of pentobarbital sodium (Abbott Laboratories, Abbott Park, IL, , USA) (45). Fetal hearts were perfused for cardiomyocyte isolation, and heart tissues were collected, snap frozen, and stored at −80°C. The fetuses studied were obtained from 11 control ewes and 14 MO ewes. Among those, 5 control and 7 MO fetuses were used for cardiomyocyte isolation, and 6 fetuses from control ewes and 7 fetuses from MO ewes were used for Western blot analysis. All animal procedures were approved by the Animal Use and Care Committee at the University of Wyoming (Laramie, WY, USA), and the sheep were housed in facilities accredited by the Association for Assessment and Accreditation of Laboratory Animal Care International.

Isolation of fetal sheep cardiomyocytes

The protocol for isolating cardiomyocytes was modified from previous reports (52–55). The fetal hearts were dissected and perfused with heparin (20,000 IU in 10 ml saline) through the coronary vessels *via* the ascending aorta followed by 10 ml of saturated KCl (34%) at room temperature. The ascending aorta was cannulated, and the fetal heart was mounted in a temperature-controlled (37°C) perfusion apparatus. After perfusion with oxygenated Ca^{2+}-free Tyrode buffer (in mM) [NaCl 125, KCl 4.5, $MgSO_4$ 1.2, NaH_2PO_4 2, 4-(2-hydroxyethyl)-1-piperazineethanesulfonic acid (HEPES) 25, pyruvate 5, and glucose 10 (pH 7.4)] and gassed with 5% CO_2 and 95% O_2 for 5 min, the fetal heart was digested for 15 min with an enzyme solution (Ca^{2+}-free Tyrode buffer with 200 U/ml collagenase and 0.1 mg/ml protease). The fetal heart was then perfused with Ca^{2+}-free Kraft-Brühe (KB) solution (in mM) [glutamic acid 74, KCl 30, KH_2PO_4 30, taurine 20, $MgSO_4$ 3, EGTA 0.5, HEPES 10, and glucose 10 (pH 7.37)] and gassed with 5% CO_2 and 95% O_2 for 10 min (~300 ml) to eliminate any remaining enzyme. After the digestion process, the fetal heart was removed from the cannula, and the LV free wall was dissected and washed with KB solution at 37°C. Individual cardiomyocytes were dispersed by cutting the LV free wall into small pieces in KB solution and filtering them through a cell strainer with a pore size of 200 μm (Thermo Fisher Scientific, Waltham, MA, USA).

Extracellular Ca^{2+} recovery

Isolated cardiomyocytes were pelleted by centrifugation at 500 rpm for 5 min. The supernatant was removed and the pellet resuspended in Ca^{2+}-free Tyrode solution. The extracellular Ca^{2+} level was gradually raised to 3, 9, 21, 45, 93, 189, 381, and 616 μM to a final concentration of 1 mM with a 10-min interval between each concentration. Cardiomyocytes were then left at 1 mM at room temperature for a half-hour, after which they were ready for mechanical and intracellular Ca^{2+} assessment.

Fetal cardiomyocyte shortening/relengthening

Rod-shaped fetal sheep cardiomyocytes with clear edges were selected for measurement of mechanical properties with a SoftEdge Myocam system (IonOptix, Milton, MA, USA). IonWizard software was used to capture changes in cardiomyocyte length during shortening and relengthening by using the SoftEdge and SarcLen acquisition modules to record cell and sarcomere length. Cardiomyocytes were placed in a C-Stim Cell MicroControls superfusion chamber system (IonOptix) on the stage of an inverted microscope (Olympus, Tokyo, Japan) and were superfused with the contractile buffer containing (in mM) NaCl 131, KCl 4, $MgCl_2$ 1, glucose 10, HEPES 10, and $CaCl_2$ 2 (pH 7.4). Cardiomyocytes were

field stimulated with an acute MyoPacer field stimulator (IonOptix) to electrically pace cellular contractions. The MyoPacer frequency setting for cardiomyocyte contractility measurement was 0.5 Hz, stimulation pulse duration was 3 ms, and voltage was 40 V. The cardiomyocyte being measured was displayed on the computer monitor *via* a MyoCam-S (IonOptix) digital acquisition camera, and the amplitude and velocities of shortening and relengthening were recorded.

Cell shortening and relengthening were assessed by using the following indices: peak shortening (PS), the shortest cell/sarcomere length of cardiomyocytes contracted on electrical stimulation, which is indicative of peak ventricular contractility; time-to-PS (TPS), the duration of myocyte shortening, which is indicative of contraction duration; time to 90% relengthening (TR_{90}), the time to reach 90% relengthening, which represents cardiomyocyte relaxation duration (90% rather than 100% relengthening was used to avoid the noisy signal present at baseline contraction); and maximum velocities of shortening (+dl/dt) and relengthening (−dl/dt), maximum slope (derivative) of the shortening and relengthening phases, which are indicators of maximum velocities of ventricular pressure increase and decrease (56, 57).

Intracellular Ca^{2+} handling

A separate cohort of cardiomyocytes was loaded with Fura-2/AM (0.5 μM) for 15 min, and fluorescence intensity was recorded with a dual-excitation fluorescence photomultiplier system (IonOptix). Cardiomyocytes were placed on an IX-70 inverted microscope (Olympus) and imaged with a Fluor ×40 oil objective. Cardiomyocytes were exposed to light emitted by a 75-W lamp and passed through either a 360- or 380-nm filter, while being stimulated at 0.5 Hz for contraction. Fluorescence emissions were detected between 480 and 520 nm, and qualitative change in Fura-2 fluorescence intensity (FFI) was inferred from the FFI ratio of the fluorescence intensity at the 2 wavelengths (360/380 nm). Fluorescence decay time (single exponential decay rate) was measured as an indicator of intracellular Ca^{2+} clearing rate (57, 58).

Wheat germ agglutinin staining

LV sections (5 μm) were stained with FITC-conjugated wheat germ agglutinin (WGA; MilliporeSigma, Burlington, MA, USA), and cardiomyocyte cross-sectional areas were calculated from randomly selected cells on a digital microscope with ImageJ (v.1.51K) software [National Institutes of Health (NIH), Bethesda, MD, USA; *https://imagej.nih.gov/ij/*] (59, 60).

Immunofluorescence staining

Paraffin-embedded sections of ventricular tissues (5 μm) were deparaffinized, and the antigen was retrieved in citrate buffer [90 mM sodium citrate, 9 mM citrate acid, and 0.5% Tween 20 (pH 6.0)]. The tissue sections were blocked in 5% bovine serum albumin for 1 h before incubation with antibodies against myosin heavy chain (MHC)-α and -β (4 μg/ml; Developmental Studies Hybridoma Bank at University of Iowa, Iowa City, IA, USA) at 4°C overnight, followed by incubation in a goat anti-mouse IgG1 Alexa Fluor 555 antibody (1:500; Thermo Fisher Scientific) at room temperature for 90 min. Tissues were visualized under a confocal microscope (Zeiss, Jena, Germany). The mean fluorescence intensity was calculated on the whole-section image with ImageJ software (NIH) (60, 61).

Western blot analysis

Fetal heart tissues were homogenized in urea-thiourea buffer [8 M urea, 2 M thiourea, 75 mM DTT, 3% SDS, 0.05% bromophenol blue, and 0.05 M Tris (pH 6.8)] as described by Guo *et al.* (62). Total protein was separated by SDS-PAGE gel and transferred onto a PVDF membrane. The membrane was probed with the following antibodies: anti-phospho-cardiac troponin I (p-cTn-I) ($Ser^{23/24}$), anti-tropomyosin, anti-sarco/endoplasmic reticulum Ca-ATPase (Serca)-2, anti-PKA, anti-phosphorylated PKA (Thr^{197}), anti-Ca^{2+}/calmodulin–dependent protein kinase II (CaMKII), anti-phosphorylated CaMKII (Thr^{286}), anti-phospholamban (PLN), and anti-β-actin (loading control) (1:1000; Cell Signaling Technology,

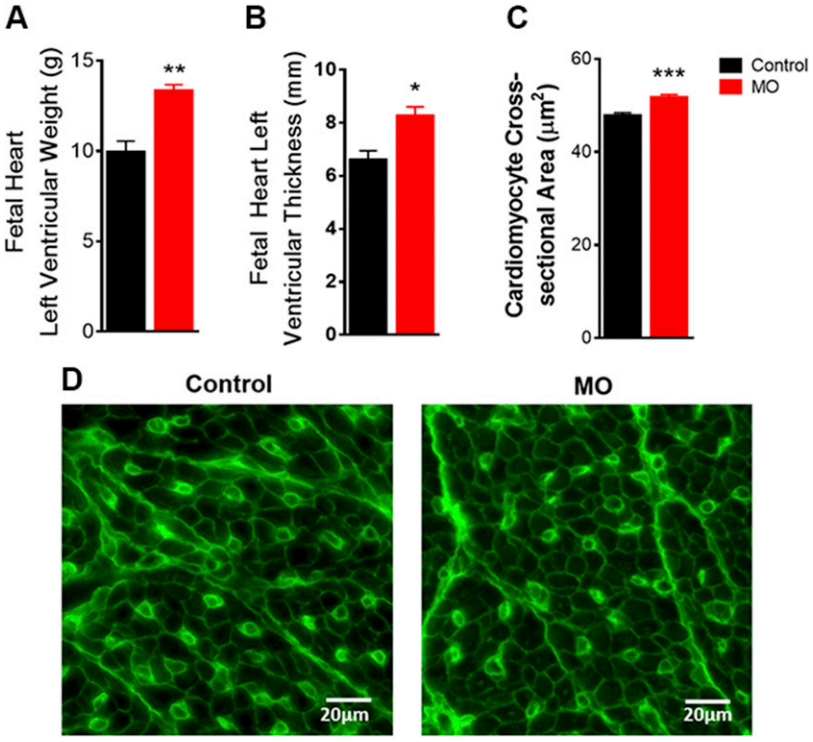

Figure 1. LV biometric properties in 0.9 gestation fetuses of control and MO mothers. *A*) LV weight ($n = 5$ control fetuses and $n = 4$ MO fetuses). *B*) LV thickness ($n = 7$ control fetuses and $n = 7$ MO fetuses). *C*) cardiomyocyte cross-sectional area, ~1000 cells (~178–258 per animal) randomly selected from 5 control and 5 MO fetal hearts. *D*) Representative images with WGA staining of cardiomyocyte cross-sectional area of LV tissues. Means ± SEM. $^*P < 0.05$, $^{**}P < 0.01$, $^{***}P < 0.001$ *vs.* control.

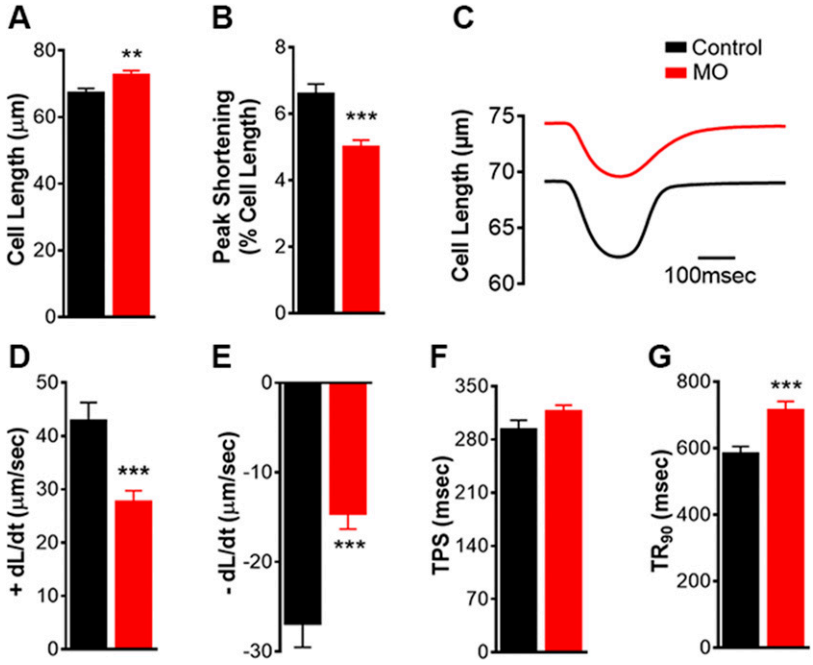

Figure 2. Mechanical contractile properties based on cell-length measurement of LV cardiomyocytes from 0.9 gestation fetuses of control and MO mothers. Resting cell length (*A*); PS (*B*); representative contractile trace (*C*); maximum velocity of shortening (*D*); maximum velocity of relengthening (*E*); TPS (*F*); and TR_{90} (*G*). Means ± SEM (n = 140 cells: 13–33 cells/animal from 5 control fetal hearts; n = 100 cells: 11–32 cells/animal from 7 MO fetal hearts). $^{**}P < 0.01$, $^{***}P < 0.001$ *vs.* control.

Danvers, MA, USA); anti-ryanodine receptor (RyR), anti-MHC-α, anti-MHC-β, anti-cTn-T, and anti-cTn-I (1:300; Developmental Studies Hybridoma Bank); anti-phosphorylated RyR-2 (Ser^{2808} and Ser^{2814}) (1:1500; Badrilla, Leeds, United Kingdom); and anti-FKBP12.6 and anti-phosphorylated PLN (Ser^{16}) (1:500; Santa Cruz Biotechnology, Dallas, TX, USA). Horseradish peroxidase–coupled secondary antibodies were used for membrane incubation. After immunoblot, the films were developed with ECL Western blot substrate (Bio-Rad, Hercules, CA, USA) and exposed to CL-Xposure film (Thermo Fisher Scientific). Density analysis of immunoblot bands was performed with NIH ImageJ by normalizing to loading control β-actin or pan proteins for phosphorylated proteins (60).

Statistical analysis

Prism software (GraphPad, La Jolla, CA, USA) was used for statistical analysis. Results are expressed as means ± SEM. Statistical significance was determined with an unpaired 2-sided *t* test analysis of differences between the 2 specified groups: control and MO. Significance was set at values of $P < 0.05$.

RESULTS

MO changes in fetal heart LV biometrics at late gestation

MO increased fetal LV free wall weight and thickness (**Fig. 1*A*, *B***). To determine hypertrophy at the cellular level, immunostaining of paraffin-embedded sections with WGA staining was performed. The cross-sectional area of LV cardiomyocytes was increased in fetuses of mothers with MO (Fig. 1*C*, *D*). These results reveal that MO leads to fetal heart hypertrophy by late gestation, suggesting that cardiac dysfunction in F1 of obese mothers later in life could originate from changes in cardiac geometry during early heart development.

MO impairs fetal cardiomyocyte contractile properties

To determine the nature of changes in cellular contractile properties, we isolated fetal cardiomyocytes from the control and MO groups. MO increased fetal cardiomyocyte resting cell length from 67.3 ± 1.3 to 72.7 ± 1.3 μm (**Fig. 2*A***), with little effect on cardiomyocyte sarcomere length (Supplemental Fig. S1*A*). Cardiomyocyte contractility based on cell-length measurements indicated that MO decreased PS and V_{max} of shortening and relengthening (±dL/dt) associated with prolonged TR_{90} (Fig. 2*B*–*G*). Contractile dynamics based on sarcomere length measurements of MO fetal cardiomyocytes showed changes similar to those obtained from cell-length measurements (Supplemental Fig. S1). These results indicate that MO increased the resting cell length of fetal cardiomyocytes, although it suppressed cardiac contractility,

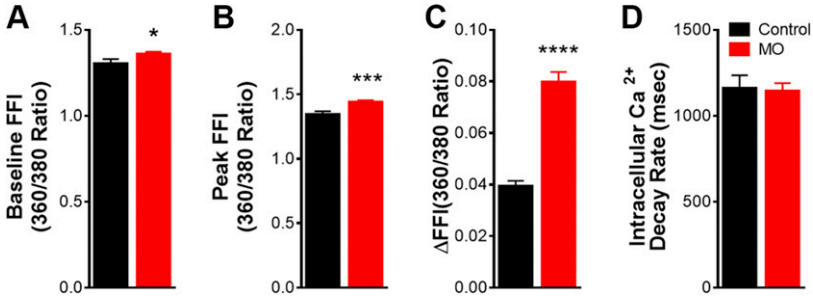

Figure 3. Intracellular Ca^{2+} transient properties of LV cardiomyocytes from 0.9 gestation fetuses of control and MO mothers. Resting FFI (*A*); peak FFI (*B*); electrically stimulated rise in FFI (ΔFFI) (*C*); and intracellular $Ca2^{+}$ decay rate (single exponential) (*D*). Means ± SEM (n = 69 cells: 11–23 cells/animal, from 4 control fetal hearts; n = 103 cells: 12–30 cells/animal, from 5 MO fetal hearts). $^{*}P < 0.05$, $^{***}P < 0.001$, $^{****}P < 0.0001$ *vs.* control.

as evidenced by a reduction of 30% in PS. Decreased PS was observed, along with slower speed of shortening and relengthening (±dL/dt) and prolonged TR_{90}. On the other hand, the duration of shortening, indicating the time from resting cell length to the maximum cell shortening of fetal cardiomyocytes, was unaffected by MO (Fig. 2*F*). Duration of TPS was shown to be unaffected, according to both the cell and sarcomere measurements (Supplemental Fig. S1*E*).

MO impairs intracellular Ca^{2+} homeostasis in fetal cardiomyocytes

To explore the possible mechanisms responsible for the impaired fetal cardiomyocyte contractile properties in response to MO, intracellular Ca^{2+} levels were assessed with the Fura-2 fluorescence technique. MO elevated resting intracellular Ca^{2+} levels from 1.31 ± 0.02 to 1.36 ± 0.01. Peak intracellular

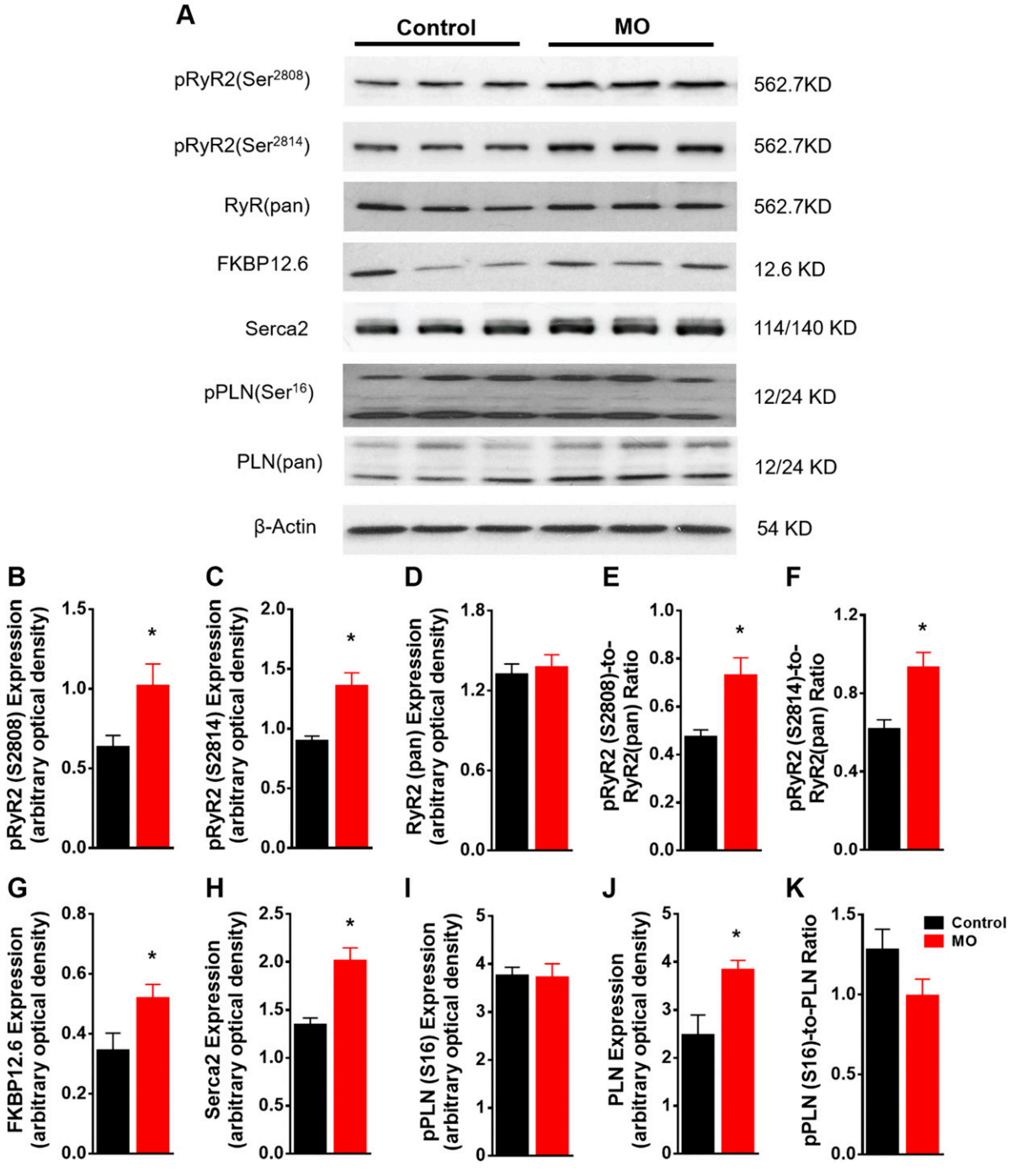

Figure 4. Western blot of Ca^{2+} pump proteins in SR from control and MO 0.9 gestation fetal heart LVs. SDS-PAGE gel image of pRyR2(Ser^{2808}), pRyR2(Ser^{2814}), RyR(pan), FKBP12.6, Serca-2, pPLN(Ser^{16}), and PLN(pan) (*A*); pRyR2(Ser^{2808}) expression (*B*); pRyR2(Ser^{2814}) expression (*C*); RyR (pan) expression (*D*); pRyR2(Ser^{2808})-to-RyR(pan) ratio (*E*); pRyR2(Ser^{2814})-to-RyR(pan) ratio (*F*); FKBP12.6 expression (*G*); Serca2 expression (*H*); pPLN(Ser^{16}) expression (*I*); PLN(pan) expression (*J*); and pPLN-to-PLN(pan) ratio (*K*). Means ± SEM. (*B–D* and *G–J*, $n = 6$ control fetal hearts and $n = 7$ MO fetal hearts, normalized to β-actin expression; *E*, *F*, and *K* normalized to relative pan protein expression). *$P < 0.05$ *vs.* control.

Ca^{2+} ratios increased from 1.34 ± 0.03 to 1.44 ± 0.01. FFI rose (ΔFFI) from 0.039 ± 0.002 to 0.080 ± 0.004 (**Fig. 3*A–C***). However, the intracellular Ca^{2+} clearance rate was unaffected by MO (Fig. 3*D*). These results revealed that MO led to elevated resting intracellular Ca^{2+} and a greater release of Ca^{2+} in response to electric stimulation (ΔFFI) in fetal cardiomyocytes, but that intracellular Ca^{2+} uptake rate was similar in MO compared with control fetal cardiomyocytes. These findings suggest that intracellular Ca^{2+} is overloaded in MO fetal cardiomyocytes, which could be a mechanism leading to impaired fetal cardiomyocyte contractile properties.

Changes in Ca^{2+}-handling proteins in fetal cardiomyocytes of obese mothers

Western blot analysis (**Fig. 4*A***) revealed similar levels in total RyR between MO and control fetal hearts. However, phosphorylation of RyR2 at Ser^{2808} and Ser^{2814} was significantly enhanced in MO fetal myocardium (Fig. 4*B–F*). Increased expression of the RyR2 binding protein FK 506 binding protein 12.6 was observed (Fig. 4*G*). Serca-2 and PLN are 2 major proteins in the Ca^{2+}-uptake pump, and changes in these proteins may impair Ca^{2+} uptake (63). Expression of Serca-2 and phosphorylated PLN (Ser^{16}) were unchanged (Fig. 4*H, I, K*). However, expression of pan PLN was increased in MO fetal myocardium (Fig. 4*J*). These results suggest that Ca^{2+} was leaking from the Ca^{2+}-release channel, but because there was no change in the Ca^{2+} uptake pump, the intracellular Ca^{2+} level in MO fetal cardiomyocytes was elevated.

Next, we examined the upstream kinases CaMKII and PKA that phosphorylate Ser^{2808} and Ser^{2814} of RyR2. MO did not affect expression of total PKA and CaMKII in the fetal myocardium, but phosphorylation of both kinases was elevated in MO fetal hearts (**Fig. 5**), suggesting that MO leads to activation of both PKA and CaMKII but not to altered total expression of these 2 kinases.

Changes in contractile and regulatory proteins in the MO fetal myocardium

To explore the effect of MO on the contractile protein Myosin and the regulatory proteins troponin and tropomyosin, we performed immunofluorescent staining with specific antibodies: anti-MHC-α and -β. MO reduced

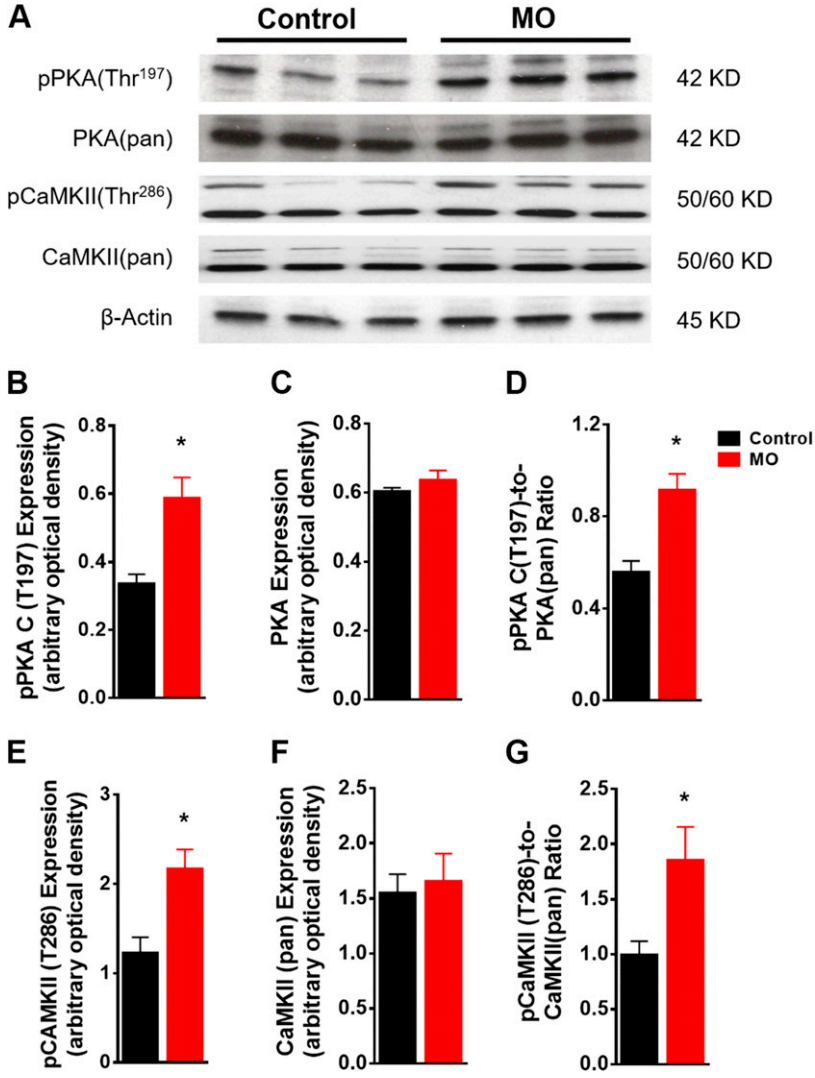

Figure 5. Western blot of kinases active in Ca^{2+} signaling in control and MO 0.9 gestation fetal heart LVs. SDS-PAGE gel image of pPKA (Thr^{197}), PKA(pan), pCaMKII(Thr^{286}) and CaMKII(pan) (*A*); pPKA(Thr^{197}) expression (*B*); PKA(pan) expression (*C*); pPKA(Thr^{197})-to-PKA(pan) ratio (*D*); pCaMKII(Thr^{286}) expression (*E*); CaMKII(pan) expression (*F*); and pCaMKII(Thr^{286})-to-CaMKII(pan) ratio (*G*). Means ± SEM. (*B*, *C*, *E*, and *F*, $n = 6$ control fetal hearts and $n = 7$ MO fetal hearts, normalized to β-actin expression; *D*, and *G* to relative pan protein expression). $^*P < 0.05$ *vs.* control.

MHC-α fluorescence intensity but increased that of MHC-β (**Fig. 6*A–D***). Furthermore, Western blot results confirmed the reduced MHC-α and elevated MHC-β protein expression in the MO fetal heart (Fig. 6*E–H*). These results suggest that MO decreases the levels of high-ATP hydrolysis MHC-α associated with fast twitch and increases the levels of low-ATP hydrolysis MHC-β associated with slow twitch. These changes indicate that MO slows fetal heart contraction, in agreement with our findings in single cardiomyocytes.

We next examined the expression and phosphorylation status of the regulatory proteins, troponin complex and tropomyosin. Western blot analysis (**Fig. 7A**) revealed that expression of cTn-T was increased by ~60%, phosphorylation of cTn-I was increased by ~130%, and cardiac tropomyosin was increased by 110% in fetal myocardium from the MO group (Fig. 7*B–F*). No changes were observed for cTn-C expression in the fetal myocardium (Fig. 7*G*). These results indicated that MO affected the composition of the myofilament regulatory troponin-tropomyosin complex.

DISCUSSION

The findings of this study indicate that MO impairs fetal myocardial contractile function, and intracellular Ca^{2+} homeostasis. The compromised cardiomyocyte contractile function and intracellular Ca^{2+} handling seen in fetuses from MO ewes were accompanied by changes in contractile and regulatory proteins. Previous studies suggested that MO programs cardiac remodeling and disrupts cardiac homeostasis in fetal sheep heart (16, 18, 25, 33, 51), although little information is available relating to activity of individual cardiomyocytes. Maternal overfeeding during early to midgestation has been reported to increase ventricular free wall weights and wall thickness in fetal sheep (49, 50). Moreover, MO induces cardiac hypertrophy in the mouse, human, and sheep fetal heart (25–27). Our findings are consistent with these earlier findings. We provide further evidence of cardiac remodeling and hypertrophy indicated by elongated single cardiomyocyte length and enlarged cardiomyocyte cross-sectional area. *In vitro*, whole-heart Langendorff studies indicated that contractile function in the MO fetal heart is compromised under high workloads (16). However, contractile profiles of individual fetal sheep cardiomyocytes have not been studied. Our results revealed that MO-reduced contractile function in fetal cardiomyocytes decreased cell shortening and slowed the speed of contraction. These findings provide important new cellular evidence of the nature of MO-induced cardiac dysfunction in single cardiomyocytes.

Intracellular Ca^{2+} release and uptake play essential roles in contractile function of the normal mammalian cardiac muscle cell (63). Two major Ca^{2+}-dependent

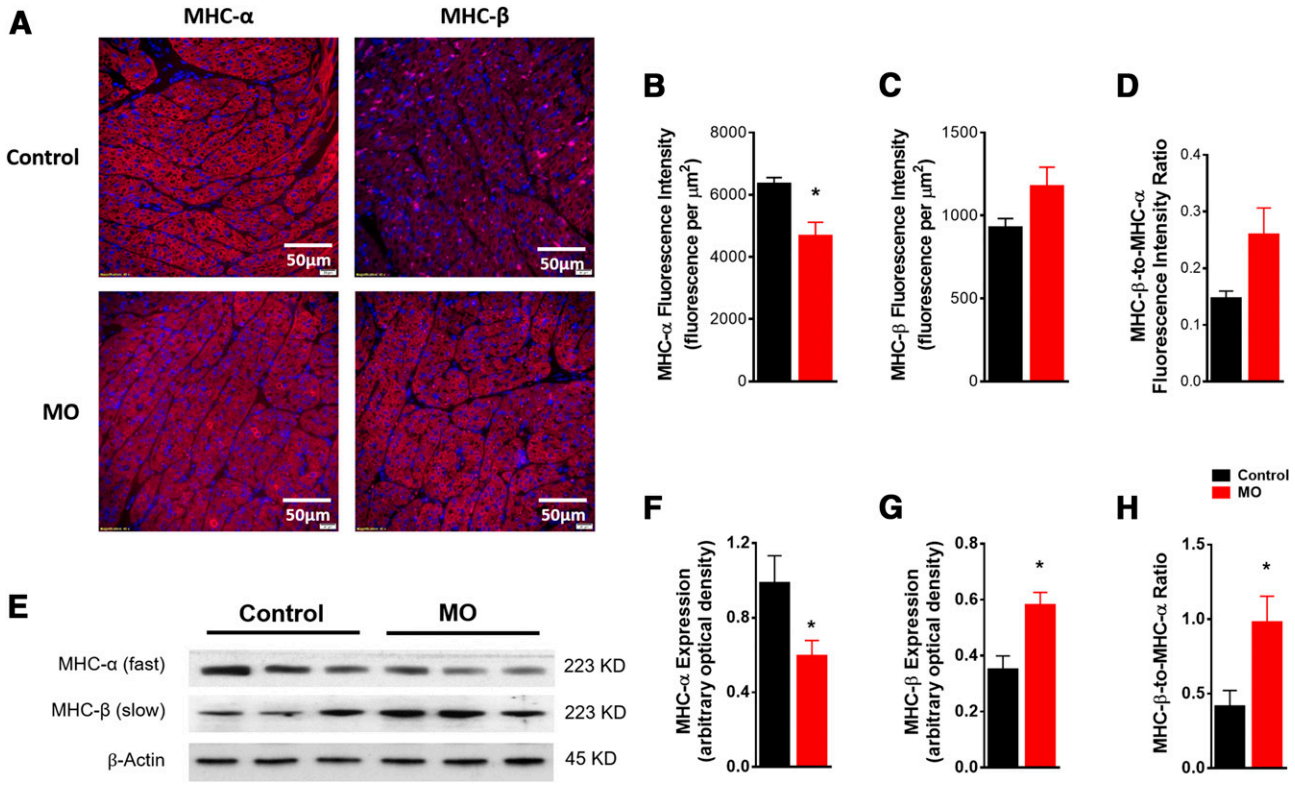

Figure 6. MHC expression in control and MO 0.9 gestation fetal heart LVs. Representative images of immunofluorescence staining of cardiac MHC-α (red), MHC-β (red) in fetal LV tissue, nucleus stained by DAPI (blue) (*A*); mean fluorescence intensity of MHC-α (*B*); mean fluorescence intensity of MHC-β (*C*); fluorescence intensity of MHC-β:MHC-α ratio (*D*); SDS-PAGE gel image of MHC-α and -β (*E*); MHC-α expression (*F*); MHC-β expression (*G*); MHC-β:MHC-α expression ratio (*H*). Means ± SEM. (*F* and *G*, $n = 6$ control fetal hearts and $n = 7$ MO fetal hearts, normalized to β-actin expression; *H*, normalized to MHC-α protein expression). *$P < 0.05$ *vs.* control.

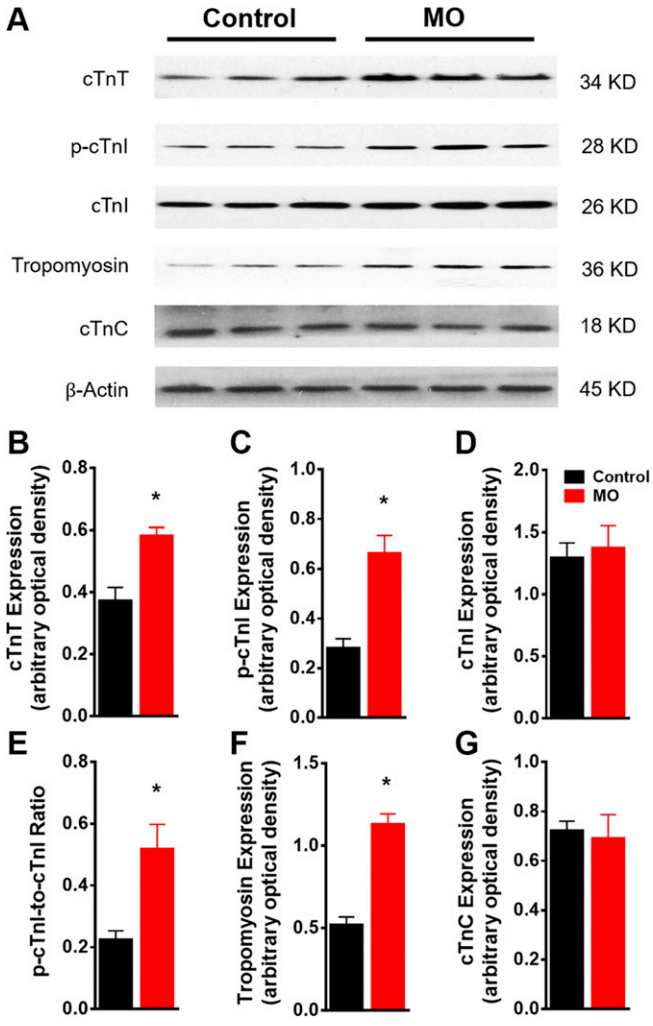

Figure 7. Western blot of troponin complex protein markers in control and MO 0.9 gestation fetal heart LVs. SDS-PAGE gel image of cTn-T, p-cTn-I, cTn-I, cardiac tropomyosin and cTn-C (*A*); cTn-T expression (*B*); p-cTn-I expression (*C*); cTn-I expression (*D*); p-cTn-I:cTn-I ratio (*E*); tropomyosin expression (*F*); and cTnC expression (*G*). Means ± SEM. (*B–D*, *F*, and *G*, $n = 6$ control fetal hearts and $n = 7$ MO fetal hearts, normalized to β-actin expression and *E*, normalized to relative pan protein expression). *$P < 0.05$ *vs.* control.

mechanisms—the availability of Ca^{2+} to the myofilaments and myofilament responsiveness to activation by intracellular Ca^{2+}—are key regulators of the cardiac contractile state (64, 65). Ca^{2+} availability is regulated by the sarcoplasmic reticulum (SR). Imbalance between release and uptake of Ca^{2+} results in altered intracellular Ca^{2+} levels. When Ca^{2+} release exceeds its uptake, cells will eventually become overloaded with Ca^{2+}, leading to cardiomyocyte contractile dysfunction (64, 66–69). The cellular measurement of Ca^{2+} showed that the resting and the peak levels were both higher in MO fetal cardiomyocytes because of increased Ca^{2+} release. However, the Ca^{2+} clearance rate was unaffected by MO. The higher intracellular Ca^{2+} would increase the time needed for Ca^{2+} reuptake into the SR in MO cardiomyocytes, which is consistent with prolonged cell relengthening time. Increased intracellular Ca^{2+} levels suggest Ca^{2+} overload in MO fetal cardiomyocytes, which may be associated with impaired activity of the Ca^{2+}-release channel. Studies have shown that phosphorylation by PKA of RyR2 at Ser^{2808} and phosphorylation by CaMKII of RyR2 at Ser^{2814} can reduce the stability of the Ca^{2+} release channel RyR2 and lead to a Ca^{2+} leak from the SR associated with cardiac contractility dysfunction and heart failure (70–74). Our data show increased activity of PKA and CaMKII and high phosphorylation levels at both Ser^{2808} and Ser^{2814} of RyR2, which further confirm impaired contractile function in MO fetal cardiomyocytes at the molecular level.

Cardiomyocyte contractility is also regulated by the sensitivity of myofilaments to Ca^{2+}. Evidence has indicated a role for MHC isoform composition and cardiac troponin in myocardial contractile dysfunction (75–80). It has been shown that the specific pattern of cardiac MHC isoform expression significantly affects cardiomyocyte contractile properties (81–85). In particular, isoform switching from MHC-α to -β has been reported as being associated with suppressed cardiac contractile function in failing hearts (75, 77, 79, 80, 82, 83). Therefore, the down-regulated MHC-α and up-regulated MHC-β seen in MO fetal hearts could lead to reduced and slower cardiomyocyte contractility. Cardiac troponin proteins play a critical role in transducing Ca^{2+} binding to initiate cardiac muscle contraction (86–88). McAuliffe and Robbins (89) have identified only 1 cTn-T isoform in the fetal sheep heart. Although several studies have been conducted on the Ca^{2+} sensitivity and cTn-T, these studies have shown that variations in isoforms of cTn-T affect Ca^{2+} sensitivity and cardiac contractility (90–92). However, there are no reports of how various conditions affect contractility in fetal sheep in the presence of only 1 form of troponin. Data presented herein, show that increased expression of cTn-T is associated with reduced cardiomyocyte contractility. Further studies are needed to determine how MO-induced upregulation of cTn-T affects the function and structure of the troponin complex, and thereby, cardiac contractility. Increased phosphorylation of cTn-I increases the Ca^{2+} necessary to achieve half-maximum myofibrillar ATPase and decreases the amount of Ca^{2+} available to myofilaments (93). Although we failed to note any change in cTn-C, the major element in the troponin complex binding Ca^{2+} to transduce mechanosensing to the myofilament, the increased phosphorylation of cTn-I in MO fetal heart could help to explain the reduced contractility, potentially by reducing enzyme activity of myofibrillar ATPase. Further studies are necessary to determine the mechanisms of MO-induced fetal cardiomyocyte Ca^{2+} insensitivity.

Another major goal of our study was to establish a reliable method to assess fetal cardiac mechanistic function at the level of the individual fetal cardiomyocyte. The challenge in mechanical assessment of single fetal cardiomyocyte function is the ability to isolate viable fetal cardiomyocytes and buffer the cells in optimal conditions to respond to field electric stimulation. Fetal sheep cardiomyocyte isolation methods have been established for over 15 yr (52), and several elegant studies have demonstrated endocrine control of the cell cycle and growth in fetal sheep cardiomyocytes (94–97). However, our data are the first, to our knowledge, on contractility of individual fetal cardiomyocytes.

There is a need to develop and refine methods to evaluate mechanisms that control fetal sheep cardiomyocyte contractility. Reported methods maintain cardiomyocytes in a Ca^{2+} free environment (52, 54, 94–96). Calcium plays a critical role in cardiac contraction (98, 99). Therefore, the isolated Ca^{2+}-free fetal sheep cardiomyocytes could not contract in response to electric stimuli. To assess the contractile function and intracellular Ca^{2+} handling, normal Ca^{2+} levels have to be restored in the fetal sheep cardiomyocyte (58, 100–102). In published studies on cardiomyocyte contractility in adult mice and rats, the concentration of extracellular Ca^{2+} increased to 1.25 mM (57–59, 103). However, different extracellular Ca^{2+} concentrations have been used in different studies: Thompson *et al.* (101) used 1.8 mM in isolated cardiomyocytes from guinea pigs, Chandrashekhar *et al.* (100) used 0.2 mM in rat cardiomyocytes, and Griffiths *et al.* (102) raised the extracellular Ca^{2+} to 2 mM in isolated rat cardiomyocytes. In our study, we first followed the Ca^{2+} recovery steps as described in Ren and Wold (58), with initial Ca^{2+} concentration as 100 μM and raised to 1.25 mM in 5 steps of double increments. However, the viability of fetal sheep cardiomyocytes decreased dramatically from ~70–20%, which indicates that the fetal sheep cardiomyocytes are very sensitive to extracellular Ca^{2+}. Because there are no reports investigating isolated fetal cardiomyocytes in other species, it remains to be determined whether there is similar sensitivity to Ca^{2+} concentrations in other experimental species, both precocial and altricial. Based on these observations of the sensitivity of the fetal sheep cardiomyocyte to Ca^{2+}, we modified the Ca^{2+} recovery procedure to start with 3 μM and ended with 1 mM with 9 gradual incremental steps. This approach helped to maintain fetal sheep cardiomyocyte viability at ~60%. The levels of Ca^{2+} in the contractile buffer also affected myocyte contractility. The conventional level of 1 mM Ca^{2+} in the contractile solution did not stimulate fetal sheep cardiomyocytes; however, in this study, 2 mM Ca^{2+} was determined to be the ideal concentration for the contraction solution. Higher Ca^{2+} concentrations (≥4 mM) in the contraction solution may reduce viability and result in the death of fetal sheep cardiomyocytes during the measurement of contractility. The Ca^{2+} concentration in the contraction solution determines the extracellular Ca^{2+} concentration during the measurement of contractile function. In our case, the working concentration of extracellular Ca^{2+} was 2 mM, which is the normal extracellular concentration of Ca^{2+} (104, 105). The methods we developed for Ca^{2+} recovery and assessment of contractility in fetal sheep cardiomyocytes showed that an extracellular Ca^{2+} level of 1 mM in the fetal myocyte maintains cell viability. In addition, we showed the effects of a working concentration of extracellular Ca^{2+} of 2 mM, which is the normal physiologic condition of cardiomyocytes. These guidelines will be of value in future studies.

In summary, our study represents a characterization of MO effects on fetal cardiomyocyte contractility. The data suggest that MO induces cardiac functional and geometric anomalies in fetal sheep hearts *via* alteration of myofilament proteins and the SR Ca^{2+} channel. In fetuses of mothers with MO, there is a fetal myocardial MHC isoform switch from the high-ATPase activity MHC-α isoform to the low-ATPase activity MHC-β, along with an altered cTn complex. This switch could be one mechanistic cause of reduced contractility in MO fetal sheep cardiomyocytes. Our results also suggest that MO disrupts intracellular Ca^{2+} homeostasis in fetal hearts by elevating phosphorylation of the SR Ca^{2+}-release channel RyR2, whereas the SR Ca^{2+}uptake channel was not affected. This conclusion is supported by our observation of intracellular Ca^{2+} transience in fetal sheep cardiomyocytes. That upstream Ca^{2+} signaling molecules of RyR2, PKA, and CaMKII were activated in the MO fetal myocardium suggests a vital role for dysfunctional cellular Ca^{2+} signaling mechanisms in the MO fetal heart (**Fig. 8**). Although further studies are needed to understand mechanisms

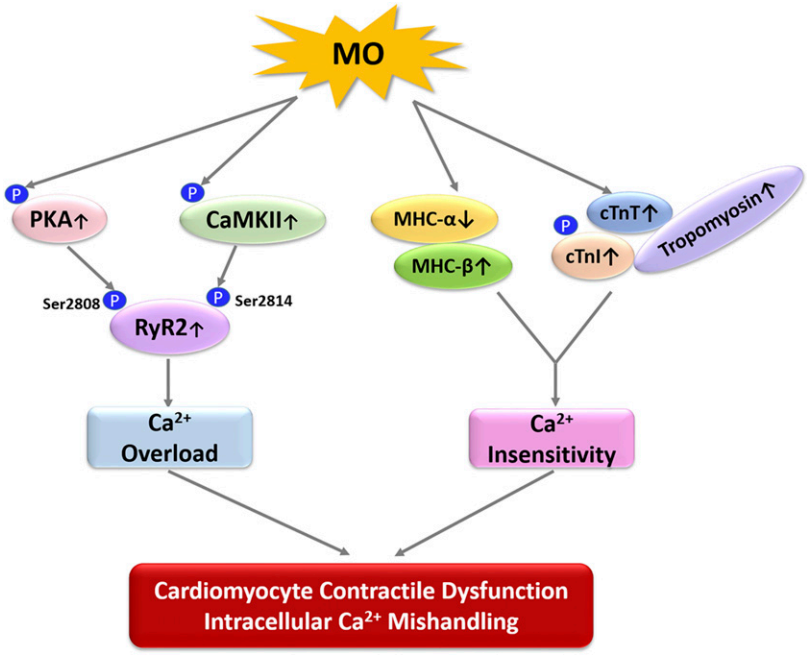

Figure 8. The signaling pathways linking MO to fetal heart contractile dysfunction. MO activates phosphorylation of PKA and CaMKII which further activate SR Ca^{2+} release channel RyR2 at Ser^{2808} and Ser^{2814}, resulting in intracellular Ca^{2+} overload. On the other hand, MO decreases MHC-α and increases MHC-β. Meanwhile, MO increases cTn-T, phosphorylation of cTn-I, and tropomyosin, which lead to Ca^{2+} insensitivity of the myofilament. We conclude that intracellular Ca^{2+} overload and insensitivity are major causes of fetal cardiomyocyte contractile dysfunction and intracellular Ca^{2+} mishandling. Up arrows: up-regulation; down arrows: down-regulation.

underlying MO-induced changes in fetal cardiac contractile function, our data provide additional mechanistic evidence at both the cellular and molecular levels which, if they persist, would contribute to programming of life course adult cardiovascular disease in F1 offspring of obese mothers. FJ

ACKNOWLEDGMENTS

The authors thank Dr. John F. Odhiambo, Dr. Adel Ghnenis, Dr. Shuyi Wang, Dr. Guorong Ruan, Dr. Zhilong Chen, Christopher Pankey, Dallas Sturdevant, and Ashley Smith (all from the University of Wyoming) for performing tissue collection and sheep necropsy; and Pan Chen (University of Wyoming) for help in obtaining immunofluorescence microscopic images of fetal sheep LV sections. The authors dedicate this work to the late Stephen P. Ford, M.D., a co-founder of the University of Wyoming Fetal Programming Center. This work was supported by National Institutes of Health (NIH), National Institute of General Medical Sciences Grant GMSP20GM103432; American Heart Association, Beginning Grant-in-Aid award to 16BGIA27790136 (to W.G.); a U.S. Department of Agriculture, National Institute of Food and Agriculture Hatch Project 1009266 (to WG); NIH, Eunice Kennedy Shriver National Institute of Child Health and Human Development Grant 1R01HD070096-01A1 (to S.P.F. and P.W.N.). The authors declare no conflicts of interest.

AUTHOR CONTRIBUTIONS

Q. Wang and W. Guo designed the experiments; Q. Wang and W. Guo analyzed and interpreted the data; Q. Wang, C. Zhu, M. Sun, and R. Maimaiti performed the experiments; S. P. Ford and J. Ren contributed new reagents or analytic tools; Q. Wang and W. Guo wrote the manuscript; and P. W. Nathanielsz and J. Ren revised the manuscript.

REFERENCES

1. WHO. (2015) Obesity and overweight. Fact sheet No. 311. World Health Organization, Geneva, Switzerland. Retrieved 7/21/2016 from http://www.who.int/mediacentre/factsheets/fs311/en/
2. Flegal, K. M., Carroll, M. D., Kit, B. K., and Ogden, C. L. (2012) Prevalence of obesity and trends in the distribution of body mass index among US adults, 1999-2010. *JAMA* **307**, 491–497
3. Ogden, C. L., Carroll, M. D., McDowell, M. A., and Flegal, K. M. (2007) Obesity among adults in the United States: no statistically significant change since 2003-2004. *NCHS Data Brief* **1**, 1–8
4. American College of Obstetricians and Gynecologists. (2005) ACOG Committee Opinion number 315, September 2005. Obesity in pregnancy. *Obstet. Gynecol.* **106**, 671–675
5. Hillemeier, M. M., Weisman, C. S., Chuang, C., Downs, D. S., McCall-Hosenfeld, J., and Camacho, F. (2011) Transition to overweight or obesity among women of reproductive age. *J. Womens Health (Larchmt.)* **20**, 703–710
6. Ramsay, J. E., Ferrell, W. R., Crawford, L., Wallace, A. M., Greer, I. A., and Sattar, N. (2002) Maternal obesity is associated with dysregulation of metabolic, vascular, and inflammatory pathways. *J. Clin. Endocrinol. Metab.* **87**, 4231–4237
7. Drake, A. J., and Reynolds, R. M. (2010) Impact of maternal obesity on offspring obesity and cardiometabolic disease risk. *Reproduction* **140**, 387–398
8. Zhang, S., Rattanatray, L., McMillen, I. C., Suter, C. M., and Morrison, J. L. (2011) Periconceptional nutrition and the early programming of a life of obesity or adversity. *Prog. Biophys. Mol. Biol.* **106**, 307–314
9. Alfaradhi, M. Z., and Ozanne, S. E. (2011) Developmental programming in response to maternal overnutrition. *Front. Genet.* **2**, 27
10. Dong, M., Zheng, Q., Ford, S. P., Nathanielsz, P. W., and Ren, J. (2013) Maternal obesity, lipotoxicity and cardiovascular diseases in offspring. *J. Mol. Cell. Cardiol.* **55**, 111–116
11. Rankin, J., Tennant, P. W., Stothard, K. J., Bythell, M., Summerbell, C. D., and Bell, R. (2010) Maternal body mass index and congenital anomaly risk: a cohort study. *Int. J. Obes.* **34**, 1371–1380; erratum: 1449
12. Zambrano, E., and Nathanielsz, P. W. (2013) Mechanisms by which maternal obesity programs offspring for obesity: evidence from animal studies. *Nutr. Rev.* **71**(Suppl 1), S42–S54
13. Lee, K. K., Raja, E. A., Lee, A. J., Bhattacharya, S., Bhattacharya, S., Norman, J. E., and Reynolds, R. M. (2015) Maternal obesity during pregnancy associates with premature mortality and major cardiovascular events in later life. *Hypertension* **66**, 938–944
14. Nicholas, L. M., Morrison, J. L., Rattanatray, L., Zhang, S., Ozanne, S. E., and McMillen, I. C. (2016) The early origins of obesity and insulin resistance: timing, programming and mechanisms. *Int. J. Obes.* **40**, 229–238
15. Dong, F., Ford, S. P., Nijland, M. J., Nathanielsz, P. W., and Ren, J. (2008) Influence of maternal undernutrition and overfeeding on cardiac ciliary neurotrophic factor receptor and ventricular size in fetal sheep. *J. Nutr. Biochem.* **19**, 409–414
16. Wang, J., Ma, H., Tong, C., Zhang, H., Lawlis, G. B., Li, Y., Zang, M., Ren, J., Nijland, M. J., Ford, S. P., Nathanielsz, P. W., and Li, J. (2010) Overnutrition and maternal obesity in sheep pregnancy alter the JNK-IRS-1 signaling cascades and cardiac function in the fetal heart. *FASEB J.* **24**, 2066–2076
17. Thornburg, K. L. (2015) The programming of cardiovascular disease. *J. Dev. Orig. Health Dis.* **6**, 366–376
18. Blackmore, H. L., Niu, Y., Fernandez-Twinn, D. S., Tarry-Adkins, J. L., Giussani, D. A., and Ozanne, S. E. (2014) Maternal diet-induced obesity programs cardiovascular dysfunction in adult male mouse offspring independent of current body weight. *Endocrinology* **155**, 3970–3980
19. Brite, J., Laughon, S. K., Troendle, J., and Mills, J. (2014) Maternal overweight and obesity and risk of congenital heart defects in offspring. *Int. J. Obes.* **38**, 878–882; erratum: 886
20. Cai, G. J., Sun, X. X., Zhang, L., and Hong, Q. (2014) Association between maternal body mass index and congenital heart defects in offspring: a systematic review. *Am. J. Obstet. Gynecol.* **211**, 91–117
21. Stothard, K. J., Tennant, P. W., Bell, R., and Rankin, J. (2009) Maternal overweight and obesity and the risk of congenital anomalies: a systematic review and meta-analysis. *JAMA* **301**, 636–650
22. Karachaliou, M., Georgiou, V., Roumeliotaki, T., Chalkiadaki, G., Daraki, V., Koinaki, S., Dermitzaki, E., Sarri, K., Vassilaki, M., Kogevinas, M., Oken, E., and Chatzi, L. (2015) Association of trimester-specific gestational weight gain with fetal growth, offspring obesity, and cardiometabolic traits in early childhood. *Am. J. Obstet. Gynecol.* **212**, 502.e501–514
23. Reynolds, R. M., Allan, K. M., Raja, E. A., Bhattacharya, S., McNeill, G., Hannaford, P. C., Sarwar, N., Lee, A. J., Bhattacharya, S., and Norman, J. E. (2013) Maternal obesity during pregnancy and premature mortality from cardiovascular event in adult offspring: follow-up of 1 323 275 person years. *BMJ* **347**, f4539
24. Ingul, C. B., Lorås, L., Tegnander, E., Eik-Nes, S. H., and Brantberg, A. (2016) Maternal obesity affects fetal myocardial function as early as in the first trimester. *Ultrasound Obstet. Gynecol.* **47**, 433–442
25. Fernandez-Twinn, D. S., Blackmore, H. L., Siggens, L., Giussani, D. A., Cross, C. M., Foo, R., and Ozanne, S. E. (2012) The programming of cardiac hypertrophy in the offspring by maternal obesity is associated with hyperinsulinemia, AKT, ERK, and mTOR activation. *Endocrinology* **153**, 5961–5971
26. Toemen, L., Gishti, O., van Osch-Gevers, L., Steegers, E. A., Helbing, W. A., Felix, J. F., Reiss, I. K., Duijts, L., Gaillard, R., and Jaddoe, V. W. (2016) Maternal obesity, gestational weight gain and childhood cardiac outcomes: role of childhood body mass index. *Int. J. Obes.* **40**, 1070–1078
27. Ghnenis, A. B., Odhiambo, J. F., McCormick, R. J., Nathanielsz, P. W., and Ford, S. P. (2017) Maternal obesity in the ewe increases cardiac ventricular expression of glucocorticoid receptors, proinflammatory cytokines and fibrosis in adult male offspring. *PLoS One* **12**, e0189977
28. Nathanielsz, P. W., Ford, S. P., Long, N. M., Vega, C. C., Reyes-Castro, L. A., and Zambrano, E. (2013) Interventions to prevent adverse fetal programming due to maternal obesity during pregnancy. *Nutr. Rev.* **71**(Suppl 1), S78–S87
29. Zambrano, E., Martínez-Samayoa, P. M., Rodríguez-González, G. L., and Nathanielsz, P. W. (2010) Dietary intervention prior to

pregnancy reverses metabolic programming in male offspring of obese rats. *J. Physiol.* **588**, 1791–1799
30. Vega, C. C., Reyes-Castro, L. A., Bautista, C. J., Larrea, F., Nathanielsz, P. W., and Zambrano, E. (2015) Exercise in obese female rats has beneficial effects on maternal and male and female offspring metabolism. *Int. J. Obes.* **39**, 712–719
31. Kirk, S. L., Samuelsson, A. M., Argenton, M., Dhonye, H., Kalamatianos, T., Poston, L., Taylor, P. D., and Coen, C. W. (2009) Maternal obesity induced by diet in rats permanently influences central processes regulating food intake in offspring. *PLoS One* **4**, e5870
32. Samuelsson, A. M., Matthews, P. A., Argenton, M., Christie, M. R., McConnell, J. M., Jansen, E. H., Piersma, A. H., Ozanne, S. E., Twinn, D. F., Remacle, C., Rowlerson, A., Poston, L., and Taylor, P. D. (2008) Diet-induced obesity in female mice leads to offspring hyperphagia, adiposity, hypertension, and insulin resistance: a novel murine model of developmental programming. *Hypertension* **51**, 383–392
33. Loche, E., Blackmore, H. L., Carpenter, A. A. M., Beeson, J. H., Pinnock, A., Ashmore, T. J., Aiken, C. E., de Almeida-Faria, J., Schoonejans, J. M., Giussani, D. A., Fernandez-Twinn, D. S., and Ozanne, S. E. (2018) Maternal diet-induced obesity programmes cardiac dysfunction in male mice independently of post-weaning diet. *Cardiovasc. Res.* **114**, 1372–1384
34. Rabadán-Diehl, C., and Nathanielsz, P. (2013) From mice to men: research models of developmental programming. *J. Dev. Orig. Health Dis.* **4**, 3–9
35. Anderson, M. S., Flowers-Ziegler, J., Das, U. G., Hay, W. W., Jr., and Devaskar, S. U. (2001) Glucose transporter protein responses to selective hyperglycemia or hyperinsulinemia in fetal sheep. *Am. J. Physiol. Regul. Integr. Comp. Physiol.* **281**, R1545–R1552
36. Anderson, M. S., He, J., Flowers-Ziegler, J., Devaskar, S. U., and Hay, W. W., Jr. (2001) Effects of selective hyperglycemia and hyperinsulinemia on glucose transporters in fetal ovine skeletal muscle. *Am. J. Physiol. Regul. Integr. Comp. Physiol.* **281**, R1256–R1263
37. Anthony, R. V., Scheaffer, A. N., Wright, C. D., and Regnault, T. R. (2003) Ruminant models of prenatal growth restriction. *Reprod. Suppl.* **61**, 183–194
38. DiGiacomo, J. E., and Hay, W. W., Jr. (1990) Effect of hypoinsulinemia and hyperglycemia on fetal glucose utilization. *Am. J. Physiol.* **259**, E506–E512
39. Dong, F., Ford, S. P., Fang, C. X., Nijland, M. J., Nathanielsz, P. W., and Ren, J. (2005) Maternal nutrient restriction during early to mid gestation up-regulates cardiac insulin-like growth factor (IGF) receptors associated with enlarged ventricular size in fetal sheep. *Growth Horm. IGF Res.* **15**, 291–299
40. Hay, W. W., Jr. (1995) Regulation of placental metabolism by glucose supply. *Reprod. Fertil. Dev.* **7**, 365–375
41. Limesand, S. W., Rozance, P. J., Smith, D., and Hay, W. W., Jr. (2007) Increased insulin sensitivity and maintenance of glucose utilization rates in fetal sheep with placental insufficiency and intrauterine growth restriction. *Am. J. Physiol. Endocrinol. Metab.* **293**, E1716–E1725
42. Wallace, J. M., Milne, J. S., Aitken, R. P., and Hay, W. W., Jr. (2007) Sensitivity to metabolic signals in late-gestation growth-restricted fetuses from rapidly growing adolescent sheep. *Am. J. Physiol. Endocrinol. Metab.* **293**, E1233–E1241
43. Hay, W. W., Jr., DiGiacomo, J. E., Meznarich, H. K., Hirst, K., and Zerbe, G. (1989) Effects of glucose and insulin on fetal glucose oxidation and oxygen consumption. *Am. J. Physiol.* **256**, E704–E713
44. National Research Council. (1985) *Nutrient Requirements of Sheep.* The National Academies Press, Washington, DC
45. Ford, S. P., Zhang, L., Zhu, M., Miller, M. M., Smith, D. T., Hess, B. W., Moss, G. E., Nathanielsz, P. W., and Nijland, M. J. (2009) Maternal obesity accelerates fetal pancreatic beta-cell but not alpha-cell development in sheep: prenatal consequences. *Am. J. Physiol. Regul. Integr. Comp. Physiol.* **297**, R835–R843
46. Zhu, M. J., Han, B., Tong, J., Ma, C., Kimzey, J. M., Underwood, K. R., Xiao, Y., Hess, B. W., Ford, S. P., Nathanielsz, P. W., and Du, M. (2008) AMP-activated protein kinase signalling pathways are down regulated and skeletal muscle development impaired in fetuses of obese, over-nourished sheep. *J. Physiol.* **586**, 2651–2664
47. Tuersunjiang, N., Odhiambo, J. F., Long, N. M., Shasa, D. R., Nathanielsz, P. W., and Ford, S. P. (2013) Diet reduction to requirements in obese/overfed ewes from early gestation prevents glucose/insulin dysregulation and returns fetal adiposity and organ development to control levels. *Am. J. Physiol. Endocrinol. Metab.* **305**, E868–E878
48. George, L. A., Uthlaut, A. B., Long, N. M., Zhang, L., Ma, Y., Smith, D. T., Nathanielsz, P. W., and Ford, S. P. (2010) Different levels of overnutrition and weight gain during pregnancy have differential effects on fetal growth and organ development. *Reprod. Biol. Endocrinol.* **8**, 75
49. Fan, X., Turdi, S., Ford, S. P., Hua, Y., Nijland, M. J., Zhu, M., Nathanielsz, P. W., and Ren, J. (2011) Influence of gestational overfeeding on cardiac morphometry and hypertrophic protein markers in fetal sheep. *J. Nutr. Biochem.* **22**, 30–37
50. Huang, Y., Yan, X., Zhao, J. X., Zhu, M. J., McCormick, R. J., Ford, S. P., Nathanielsz, P. W., Ren, J., and Du, M. (2010) Maternal obesity induces fibrosis in fetal myocardium of sheep. *Am. J. Physiol. Endocrinol. Metab.* **299**, E968–E975
51. Kandadi, M. R., Hua, Y., Zhu, M., Turdi, S., Nathanielsz, P. W., Ford, S. P., Nair, S., and Ren, J. (2013) Influence of gestational overfeeding on myocardial proinflammatory mediators in fetal sheep heart. *J. Nutr. Biochem.* **24**, 1982–1990
52. Barbera, A., Giraud, G. D., Reller, M. D., Maylie, J., Morton, M. J., and Thornburg, K. L. (2000) Right ventricular systolic pressure load alters myocyte maturation in fetal sheep. *Am. J. Physiol. Regul. Integr. Comp. Physiol.* **279**, R1157–R1164
53. Morrison, J. L., Botting, K. J., Dyer, J. L., Williams, S. J., Thornburg, K. L., and McMillen, I. C. (2007) Restriction of placental function alters heart development in the sheep fetus. *Am. J. Physiol. Regul. Integr. Comp. Physiol.* **293**, R306–R313
54. Sundgren, N. C., Giraud, G. D., Schultz, J. M., Lasarev, M. R., Stork, P. J., and Thornburg, K. L. (2003) Extracellular signal-regulated kinase and phosphoinositol-3 kinase mediate IGF-1 induced proliferation of fetal sheep cardiomyocytes. *Am. J. Physiol. Regul. Integr. Comp. Physiol.* **285**, R1481–R1489
55. Wang, K. C., Brooks, D. A., Botting, K. J., and Morrison, J. L. (2012) IGF-2R-mediated signaling results in hypertrophy of cultured cardiomyocytes from fetal sheep. *Biol. Reprod.* **86**, 183
56. Ren, J., Privratsky, J. R., Yang, X., Dong, F., and Carlson, E. C. (2008) Metallothionein alleviates glutathione depletion-induced oxidative cardiomyopathy in murine hearts. *Crit. Care Med.* **36**, 2106–2116
57. Wang, Q., Yang, L., Hua, Y., Nair, S., Xu, X., and Ren, J. (2014) AMP-activated protein kinase deficiency rescues paraquat-induced cardiac contractile dysfunction through an autophagy-dependent mechanism. *Toxicol. Sci.* **142**, 6–20
58. Ren, J., and Wold, L. E. (2001) Measurement of cardiac mechanical function in isolated ventricular myocytes from rats and mice by computerized video-based imaging. *Biol. Proced. Online* **3**, 43–53
59. Wang, Q., and Ren, J. (2016) mTOR-independent autophagy inducer trehalose rescues against insulin resistance-induced myocardial contractile anomalies: role of p38 MAPK and Foxo1. *Pharmacol. Res.* **111**, 357–373
60. Schneider, C. A., Rasband, W. S., and Eliceiri, K. W. (2012) NIH Image to ImageJ: 25 years of image analysis. *Nat. Methods* **9**, 671–675
61. Li, H., Zhong, Y., Wang, Z., Gao, J., Xu, J., Chu, W., Zhang, J., Fang, S., and Du, S. J. (2013) Smyd1b is required for skeletal and cardiac muscle function in zebrafish. *Mol. Biol. Cell* **24**, 3511–3521
62. Guo, W., Schafer, S., Greaser, M. L., Radke, M. H., Liss, M., Govindarajan, T., Maatz, H., Schulz, H., Li, S., Parrish, A. M., Dauksaite, V., Vakeel, P., Klaassen, S., Gerull, B., Thierfelder, L., Regitz-Zagrosek, V., Hacker, T. A., Saupe, K. W., Dec, G. W., Ellinor, P. T., MacRae, C. A., Spallek, B., Fischer, R., Perrot, A., Özcelik, C., Saar, K., Hubner, N., and Gotthardt, M. (2012) RBM20, a gene for hereditary cardiomyopathy, regulates titin splicing. *Nat. Med.* **18**, 766–773
63. Barry, W. H., and Bridge, J. H. (1993) Intracellular calcium homeostasis in cardiac myocytes. *Circulation* **87**, 1806–1815
64. Morgan, J. P. (1991) Abnormal intracellular modulation of calcium as a major cause of cardiac contractile dysfunction. *N. Engl. J. Med.* **325**, 625–632
65. Guo, W., Zhu, C., Yin, Z., Wang, Q., Sun, M., Cao, H., and Greaser, M. L. (2018) Splicing factor RBM20 regulates transcriptional network of titin associated and calcium handling genes in the heart. *Int. J. Biol. Sci.* **14**, 369–380
66. Vassalle, M., and Lin, C. I. (2004) Calcium overload and cardiac function. *J. Biomed. Sci.* **11**, 542–565
67. Josephson, R. A., Silverman, H. S., Lakatta, E. G., Stern, M. D., and Zweier, J. L. (1991) Study of the mechanisms of hydrogen peroxide and hydroxyl free radical-induced cellular injury and calcium overload in cardiac myocytes. *J. Biol. Chem.* **266**, 2354–2361

68. Kusuoka, H., Porterfield, J. K., Weisman, H. F., Weisfeldt, M. L., and Marban, E. (1987) Pathophysiology and pathogenesis of stunned myocardium. Depressed Ca2+ activation of contraction as a consequence of reperfusion-induced cellular calcium overload in ferret hearts. *J. Clin. Invest.* **79**, 950–961
69. Clusin, W. T., Buchbinder, M., and Harrison, D. C. (1983) Calcium overload, "injury" current, and early ischaemic cardiac arrhythmias–a direct connection. *Lancet* **1**, 272–274
70. Bers, D. M. (2006) Cardiac ryanodine receptor phosphorylation: target sites and functional consequences. *Biochem. J.* **396**, e1–e3
71. Uchinoumi, H., Yang, Y., Oda, T., Li, N., Alsina, K. M., Puglisi, J. L., Chen-Izu, Y., Cornea, R. L., Wehrens, X. H. T., and Bers, D. M. (2016) CaMKII-dependent phosphorylation of RyR2 promotes targetable pathological RyR2 conformational shift. *J. Mol. Cell. Cardiol.* **98**, 62–72
72. Ai, X., Curran, J. W., Shannon, T. R., Bers, D. M., and Pogwizd, S. M. (2005) Ca2+/calmodulin-dependent protein kinase modulates cardiac ryanodine receptor phosphorylation and sarcoplasmic reticulum Ca2+ leak in heart failure. *Circ. Res.* **97**, 1314–1322
73. Kushnir, A., Shan, J., Betzenhauser, M. J., Reiken, S., and Marks, A. R. (2010) Role of CaMKIIdelta phosphorylation of the cardiac ryanodine receptor in the force frequency relationship and heart failure. *Proc. Natl. Acad. Sci. United States* **107**, 10274–10279
74. Wehrens, X. H. T., Lehnart, S. E., Reiken, S., Vest, J. A., Wronska, A., and Marks, A. R. (2006) Ryanodine receptor/calcium release channel PKA phosphorylation: a critical mediator of heart failure progression. *Proc. Natl. Acad. Sci. United States* **103**, 511–518
75. Gupta, M., Sueblinvong, V., Raman, J., Jeevanandam, V., and Gupta, M. P. (2003) Single-stranded DNA-binding proteins PURalpha and PURbeta bind to a purine-rich negative regulatory element of the alpha-myosin heavy chain gene and control transcriptional and translational regulation of the gene expression. Implications in the repression of alpha-myosin heavy chain during heart failure. *J. Biol. Chem.* **278**, 44935–44948
76. Ku, P. M., Chen, L. J., Liang, J. R., Cheng, K. C., Li, Y. X., and Cheng, J. T. (2011) Molecular role of GATA binding protein 4 (GATA-4) in hyperglycemia-induced reduction of cardiac contractility. *Cardiovasc. Diabetol.* **10**, 57
77. Lowes, B. D., Minobe, W., Abraham, W. T., Rizeq, M. N., Bohlmeyer, T. J., Quaife, R. A., Roden, R. L., Dutcher, D. L., Robertson, A. D., Voelkel, N. F., Badesch, D. B., Groves, B. M., Gilbert, E. M., and Bristow, M. R. (1997) Changes in gene expression in the intact human heart. Downregulation of alpha-myosin heavy chain in hypertrophied, failing ventricular myocardium. *J. Clin. Invest.* **100**, 2315–2324
78. Malhotra, A., Lopez, M. C., and Nakouzi, A. (1995) Troponin subunits contribute to altered myosin ATPase activity in diabetic cardiomyopathy. *Mol. Cell. Biochem.* **151**, 165–172
79. Nakao, K., Minobe, W., Roden, R., Bristow, M. R., and Leinwand, L. A. (1997) Myosin heavy chain gene expression in human heart failure. *J. Clin. Invest.* **100**, 2362–2370
80. Sucharov, C. C., Helmke, S. M., Langer, S. J., Perryman, M. B., Bristow, M., and Leinwand, L. (2004) The Ku protein complex interacts with YY1, is up-regulated in human heart failure, and represses alpha myosin heavy-chain gene expression. *Mol. Cell. Biol.* **24**, 8705–8715
81. Lompré, A. M., Nadal-Ginard, B., and Mahdavi, V. (1984) Expression of the cardiac ventricular alpha- and beta-myosin heavy chain genes is developmentally and hormonally regulated. *J. Biol. Chem.* **259**, 6437–6446
82. Miyata, S., Minobe, W., Bristow, M. R., and Leinwand, L. A. (2000) Myosin heavy chain isoform expression in the failing and nonfailing human heart. *Circ. Res.* **86**, 386–390
83. Reiser, P. J., Portman, M. A., Ning, X. H., and Schomisch Moravec, C. (2001) Human cardiac myosin heavy chain isoforms in fetal and failing adult atria and ventricles. *Am. J. Physiol. Heart Circ. Physiol.* **280**, H1814–H1820
84. Schiaffino, S., and Reggiani, C. (1996) Molecular diversity of myofibrillar proteins: gene regulation and functional significance. *Physiol. Rev.* **76**, 371–423
85. Weiss, A., and Leinwand, L. A. (1996) The mammalian myosin heavy chain gene family. *Annu. Rev. Cell Dev. Biol.* **12**, 417–439
86. Reiffert, S. U., Jaquet, K., Heilmeyer, L. M., Jr., and Herberg, F. W. (1998) Stepwise subunit interaction changes by mono- and bisphosphorylation of cardiac troponin I. *Biochemistry* **37**, 13516–13525
87. Solaro, R. J., Rosevear, P., and Kobayashi, T. (2008) The unique functions of cardiac troponin I in the control of cardiac muscle contraction and relaxation. *Biochem. Biophys. Res. Commun.* **369**, 82–87
88. Yin, Z., Ren, J., and Guo, W. (2015) Sarcomeric protein isoform transitions in cardiac muscle: a journey to heart failure. *Biochim. Biophys. Acta* **1852**, 47–52
89. McAuliffe, J. J., and Robbins, J. (1991) Troponin T expression in normal and pressure-loaded fetal sheep heart. *Pediatr. Res.* **29**, 580–585
90. Gomes, A. V., Venkatraman, G., Davis, J. P., Tikunova, S. B., Engel, P., Solaro, R. J., and Potter, J. D. (2004) Cardiac troponin T isoforms affect the Ca (2+) sensitivity of force development in the presence of slow skeletal troponin I: insights into the role of troponin T isoforms in the fetal heart. *J. Biol. Chem.* **279**, 49579–49587
91. Gomes, A. V., Guzman, G., Zhao, J., and Potter, J. D. (2002) Cardiac troponin T isoforms affect the Ca2+ sensitivity and inhibition of force development. Insights into the role of troponin T isoforms in the heart. *J. Biol. Chem.* **277**, 35341–35349
92. Anderson, P. A., Greig, A., Mark, T. M., Malouf, N. N., Oakeley, A. E., Ungerleider, R. M., Allen, P. D., and Kay, B. K. (1995) Molecular basis of human cardiac troponin T isoforms expressed in the developing, adult, and failing heart. *Circ. Res.* **76**, 681–686
93. Robertson, S. P., Johnson, J. D., Holroyde, M. J., Kranias, E. G., Potter, J. D., and Solaro, R. J. (1982) The effect of troponin I phosphorylation on the Ca2+-binding properties of the Ca2+-regulatory site of bovine cardiac troponin. *J. Biol. Chem.* **257**, 260–263
94. Giraud, G. D., Louey, S., Jonker, S., Schultz, J., and Thornburg, K. L. (2006) Cortisol stimulates cell cycle activity in the cardiomyocyte of the sheep fetus. *Endocrinology* **147**, 3643–3649
95. Jonker, S. S., Faber, J. J., Anderson, D. F., Thornburg, K. L., Louey, S., and Giraud, G. D. (2007) Sequential growth of fetal sheep cardiac myocytes in response to simultaneous arterial and venous hypertension. *Am. J. Physiol. Regul. Integr. Comp. Physiol.* **292**, R913–R919
96. Jonker, S. S., Zhang, L., Louey, S., Giraud, G. D., Thornburg, K. L., and Faber, J. J. (2007) Myocyte enlargement, differentiation, and proliferation kinetics in the fetal sheep heart. *J. Appl. Physiol.* **102**, 1130–1142
97. Sundgren, N. C., Giraud, G. D., Stork, P. J., Maylie, J. G., and Thornburg, K. L. (2003) Angiotensin II stimulates hyperplasia but not hypertrophy in immature ovine cardiomyocytes. *J. Physiol.* **548**, 881–891
98. Katz, A. M., and Lorell, B. H. (2000) Regulation of cardiac contraction and relaxation. *Circulation* **102** (20 Suppl 4), IV69–IV74
99. Kitazawa, T. (1984) Effect of extracellular calcium on contractile activation in guinea-pig ventricular muscle. *J. Physiol.* **355**, 635–659
100. Chandrashekhar, Y., Prahash, A. J., Sen, S., Gupta, S., and Anand, I. S. (1999) Cardiomyocytes from hearts with left ventricular dysfunction after ischemia-reperfusion do not manifest contractile abnormalities. *J. Am. Coll. Cardiol.* **34**, 594–602
101. Thompson, M., Kliewer, A., Maass, D., Becker, L., White, D. J., Bryant, D., Arteaga, G., Horton, J., and Giroir, B. P. (2000) Increased cardiomyocyte intracellular calcium during endotoxin-induced cardiac dysfunction in guinea pigs. *Pediatr. Res.* **47**, 669–676
102. Griffiths, E. J. (2000) Calcium handling and cell contraction in rat cardiomyocytes depleted of intracellular magnesium. *Cardiovasc. Res.* **47**, 116–123
103. Norby, F. L., Wold, L. E., Duan, J., Hintz, K. K., and Ren, J. (2002) IGF-I attenuates diabetes-induced cardiac contractile dysfunction in ventricular myocytes. *Am. J. Physiol. Endocrinol. Metab.* **283**, E658–E666
104. Klabunde, R. E. (2010) Sodium-calcium exchange in cardiac cells, in *Cardiovascular Physiology Concepts*, Retrieved 2/5/2017 from http://www.cvphysiology.com/Cardiac%20Function/CF023.htm
105. Higgins, T. J. C., Allsopp, D., and Bailey, P. J. (1980) The effect of extracellular calcium concentration and Ca-antagonist drugs on enzyme release and lactate production by anoxic heart cell cultures. *J. Mol. Cell. Cardiol.* **12**, 909–927

Received for publication May 17, 2018.
Accepted for publication September 10, 2018.